Biochimica et Biophysica Acta 1827 (2013) 355–364

Contents lists available at SciVerse ScienceDirect

Biochimica et Biophysica Acta

journal homepage: www.elsevier.com/locate/bbabio

The negative feedback molecular mechanism which regulates excitation level in the plant photosynthetic complex LHCII: Towards identification of the energy dissipative state

Monika Zubik, Rafal Luchowski, Michal Puzio, Ewa Janik, Joanna Bednarska, Wojciech Grudzinski, Wieslaw I. Gruszecki *

Department of Biophysics, Institute of Physics, Maria Curie-Sklodowska University, 20-031 Lublin, Poland

ARTICLE INFO

Article history:
Received 26 June 2012
Received in revised form 19 November 2012
Accepted 26 November 2012
Available online 3 December 2012

Keywords:
Photosynthesis
Photoprotection
Xanthophyll
Fluorescence quenching
LHCII

ABSTRACT

Overexcitation of the photosynthetic apparatus is potentially dangerous because it can cause oxidative damage. Photoprotection realized via the feedback de-excitation in the pigment–protein light-harvesting complex LHCII, embedded in the chloroplast lipid environment, was studied with use of the steady-state and time-resolved fluorescence spectroscopy techniques. Illumination of LHCII results in the pronounced singlet excitation quenching, demonstrated by decreased quantum yield of the chlorophyll *a* fluorescence and shortening of the fluorescence lifetimes. Analysis of the 77 K chlorophyll *a* fluorescence emission spectra reveals that the light-driven excitation quenching in LHCII is associated with the intensity increase of the spectral band in the region of 700 nm, relative to the principal band at 680 nm. The average chlorophyll *a* fluorescence lifetime at 700 nm changes drastically upon temperature decrease: from 1.04 ns at 300 K to 3.63 ns at 77 K. The results of the experiments lead us to conclude that: (i) the 700 nm band is associated with the inter-trimer interactions which result in the formation of the chlorophyll low-energy states acting as energy traps and non-radiative dissipation centers; (ii) the Arrhenius analysis, supported by the results of the FTIR measurements, suggests that the photo-reaction can be associated with breaking of hydrogen bonds. Possible involvement of photo-isomerization of neoxanthin, reported previously (Biochim. Biophys. Acta 1807 (2011) 1237-1243) in generation of the low-energy traps in LHCII is discussed.

1. Introduction

Live on the Earth is driven by energy of sunlight and photosynthesis is the only mechanism, developed during the evolution, to convert the energy of light to the forms which can be directly utilized by living organisms [1]. In principle, the photosynthetic apparatus works as a "quantum counter" and its fluent and effective operation depends on activity of several pigment–protein light-harvesting complexes which collect light excitations and transfer them towards the photosynthetic reaction centers. The major light-harvesting pigment–protein complex of plants, LHCII, is the most abundant membrane protein, comprising more than half of the chlorophyll pool in the biosphere [2,3]. On the other hand, excitation of the photosynthetic apparatus, over the level which can be instantly utilized by the photochemical reactions, results in generation of the reactive oxygen species, which is potentially dangerous because it can cause oxidative damage. Quenching of excessive excitations in the photosynthetic apparatus is therefore a vital regulatory activity protecting organisms against light-induced degradation. Molecular mechanisms of such regulation are not fully understood and are the subject of very intense study and debate [4–6]. Isolated LHCII is a suitable model to study overexcitation and photoprotection at the molecular level since energy transfer out of the complex, towards the photosynthetic reaction centers, does not take place and cannot decrease excitation density, therefore the complex can be considered as subjected to overexcitation conditions. Several molecular mechanisms have been reported to operate in the antenna complexes to quench excessive excitations. Among those mechanisms are the formation of chlorophyll-carotenoid [7,8] and chlorophyll–chlorophyll [9,10] charge transfer states, localized on energy scale below the Q_y level of chlorophyll *a*, thus enable of quenching of excessive chlorophyll excitations. Another reported mechanism is based upon the light-induced twist in the configuration of the LHCII-bound xanthophyll neoxanthin which induces a change in conformation of LHCII, which opens a channel for energy dissipation by energy transfer from chlorophyll *a* to the low-lying excited state of a carotenoid identified as one of the two luteins [11].

LHCII is an antenna complex comprising relatively high number of photosynthetic pigments: 14 chlorophylls and 4 xanthophylls per monomer [2,3]. The local concentration of chlorophyll in the complex

* Corresponding author. Tel.: +48 81 537 62 52; fax: +48 81 537 61 91.
E-mail address: wieslaw.gruszecki@umcs.pl (W.I. Gruszecki).

0005-2728/$ – see front matter © 2012 Elsevier B.V. All rights reserved.
http://dx.doi.org/10.1016/j.bbabio.2012.11.013

is extremely high and corresponds to ca. 0.3 M [12]. Such a high pigment concentration, combined with various orientation of individual porphyrin rings (and in consequence the dipole transitions), promotes the antenna function. On the other hand, total singlet excitation quenching due to the, so called, "concentration quenching" can be expected at such a high chlorophyll concentration [13]. Fortunately for photosynthesis, the fixed positions of the pigments in the protein pockets restricts both diffusion-limited quenching processes and the relatively weak excitonic interactions between the pigments [3]. The last restriction does not lead to the formation of low-energy states which can potentially act as energy traps via quenching the Q_y antenna-active chlorophyll *a* state. At the same time, the neighboring pigments within the LHCII monomer are close enough to be involved in the Dexter type excitation energy transfer [2,3]. Any disturbance of such a system, precisely selected during the evolution, results in the chlorophyll singlet excitation quenching in LHCII, which can be observed as a decrease in the fluorescence yield of chlorophyll *a*. A spectacular chlorophyll *a* fluorescence quenching in LHCII can be evoked by increasing a hydrostatic pressure [14] or by inducing aggregation of the monomeric or trimeric complexes [15]. On the other hand, the fluorescence quenching in LHCII was also observed in the absence of the complex aggregation [16] and even in a single LHCII trimer [17], as studied by a single molecule fluorescence spectroscopy. In the case of the aggregation-induced excitation quenching in LHCII, it is most probable that the intermolecular interactions of peripheral chlorophylls lead to formation of low-energy levels able to act as energy traps responsible for thermal dissipation [9,10].

Interestingly, Jennings et al. reported light-induced and dark-reversible singlet excitation quenching in isolated LHCII, which may act as a negative feedback de-excitation mechanism [18]. This mechanism was studied extensively in the past [19–22]. In the present work we make an attempt to identify the energy state associated with the dissipative quenching.

2. Materials and methods

2.1. Materials

LHCII was isolated from fresh spinach leaves according to Krupa et al. [23]. The complex's integrity and purity were confirmed by means of electrophoresis, HPLC, and mass spectrometry as described previously [24]. The protein was suspended in the Tricine buffer (20 mM, pH 7.6, containing 10 mM KCl). All the chemicals used in the preparation of buffer solution were purchased from Sigma Chem. Co. (USA). Monogalactosyldiacylglycerol (MGDG) and Digalactosyldiacylglycerol (DGDG) used for sample preparation were purchased from Lipid Products Company (UK). Water used for experiments was ultrapure grade (specific resistivity 18.2 MΩcm), purified with a Milli-Q system from Millipore (France). All other chemicals (analytical grade) were obtained from standard vendors.

2.2. Sample preparation

Our experience shows that the lipid environment is crucial for the system plasticity manifested by formation of supramolecular structures of LHCII, in agreement to the original reports by Simidjiev et al. [25,26]. According to this, LHCII samples were prepared as lamellar fragments of lipid membranes (see Fig. S1 of the Supplementary data). Samples containing LHCII embedded into the chloroplast lipid environment were prepared according to the following protocol. The glass test tubes containing a lipid film (MGDG and DGDG in molar ratio 2:1) deposited via evaporation under a stream of gaseous nitrogen, from the stock solution in chloroform, were incubated for 30 min under reduced pressure (less than 10^{-5} bar) in order to remove the remaining solvent. Purified LHCII suspended in the buffer containing 0.1 % n-dodecyl-β-D-maltoside (DM) was transferred to glass test tubes containing deposited lipid film and sonicated for 30 min with ultrasonic bath. The molar ratio of lipids:LHCII was as 200:1. The detergent was removed from the suspension by incubation with Biobeads adsorbent (Bio-Rad Laboratories, USA) at 4 °C for 12 hours. The LHCII-containing lipid membranes were separated from the detergent-free suspension by centrifugation (10 min at 11,200 ×*g*, 5 °C). The pellet was collected and resuspended in the buffer to reach the absorbance level 0.1 in the red band absorption maximum. To prevent photo-oxidation of LHCII-bound pigments, the samples were deoxygenated by bubbling with a gaseous argon for 10 min, directly before the experiments. The applied procedure yields formation of lamellar membrane fragments, although formation of a certain fraction of large liposomes may not be excluded. A transmission microscope image of the structures formed typically during the preparation is presented in Fig. S1.

2.3. Partial extraction of neoxanthin from LHCII

Samples containing LHCII with reduced neoxanthin concentration, embedded in the chloroplast lipid environment, were prepared according to the general procedure described above with slight modification. Before removing of the detergent the samples were supplemented with pentane (2:1, v/v; the molar fraction of pentane: LHCII monomer was as 6×10^5:1) and vigorously vortexed for 30 min. The pentane fraction appeared as a supernatant and was removed from the suspension after centrifugation (8 min at 11,200 ×*g*, 5 °C). Chromatographic analysis has proven partial and selective extraction of neoxanthin, without affecting fractions of the other group of pigments in LHCII. Approximately 10% neoxanthin was removed from the protein in course of the extraction procedure applied. A fraction of removed neoxanthin can be higher by increasing of a concentration of pentane but we have noticed additionally a certain extraction of violaxanthin and chlorophylls under such conditions.

High performance liquid chromatography (HPLC) analyses were carried out on a C-18 coated, phase-reserved column from Hichrom Ltd. (length 250 mm, internal diameter 4.6 mm) with the following solvent system: acetonitrile/methanol/water (72:8:3, v/v), used as a mobile phase. The HPLC elution rate was 0.8 ml/min. A diode-array Hewlett-Packard spectrophotometer, model HP 8453, was used as a detector, to record absorption spectra between 200 and 800 nm, in 10 s intervals.

2.4. Spectroscopic measurements

Light-driven fluorescence quenching kinetics were recorded with Cary Eclipse fluorescence spectrophotometer (Varian Inc., Australia) with modulated light excitation at 635 nm (0.18 μmol photons m^{-2} s^{-1}, excitation and emission slits set to band-widths of 20 nm and 5 nm, respectively). During measurements the samples were continuously stirred with a magnetic stirrer and the temperature was controlled by a thermostat. Light-driven chlorophyll *a* fluorescence quenching in LHCII-containing samples was induced by illumination with continuous light coming from a halogen illuminator combined with the band-pass interference filter (centered at 450 nm, band width 80 nm, Melles Griot, USA, light intensity 500 μmol photons m^{-2} s^{-1}). The fluorescence emission induced by illumination with continuous light was not detected by the spectrofluorometer (which detects selectively only a fluorescence signal characterized by the modulation frequency identical with the probing excitation light beam). The low temperature (77 K) fluorescence emission spectra were recorded with the system as already described previously [27]. Fluorescence emission analyses in a wide range of temperatures (80 K–310 K) with excitation at 642 nm were done using FluoTime 300 spectrometer (PicoQuant, Germany) with an Optistat DN2 Cryostat (Oxford Instruments, UK). The samples to be measured in a frozen state were diluted in buffer-glycerol (1:2, v:v).

Fluorescence decays (lifetime spectra) were recorded with FluoTime 300 spectrometer (PicoQuant, Germany). Excitation was at 470 nm and 642 nm with 20 MHz frequency of pulses from solid state laser respectively LDH-P-C-470 and LDH-P-635, with pulse width 70 ps and detection performed with micro-channel plate and time-correlated single photon counting system PicoHarp 300. Time-decay analyses were performed with FluoFit Pro v 4.5.3.0 (PicoQuant, Germany). Fluorescence intensity decays were analyzed by reconvolution with the instrument response function and analyzed as a sum of experimental terms.

Infrared absorption spectra were recorded at 77 K with the Fourier-transform infrared (FTIR) spectrometer, model Vector 33 from Bruker (Germany). Before measurements (40 min) and during all measurements the instrument was purged with dry argon. The attenuated total reflection (ATR) configuration was used with a 10-reflections ZnSe crystal (45° cut). Typically, 10 interferograms were collected, averaged and Fourier transformed [28]. Absorption spectra in the region between 4000 and 600 cm^{-1}, at a resolution of one data point every 4 cm^{-1}, were obtained using a clean crystal as the background. ATR crystals were cleaned with organic solvents.

Spectral analyses were performed with application of the Grams/AI software from ThermoGalactic (USA). All kind of spectroscopic measurements have been repeated at least five times and the effects presented were found to be highly reproducible.

2.5. Molecular modeling

Interaction of LHCII trimers was analyzed and visualized with VMD software support (http://www.ks.uiuc.edu/Research/vmd/) [29]. VMD has been developed, with NIH support, by the Theoretical and Computational Biophysics group at the Beckman Institute, University of Illinois at Urbana-Champaign. LHCII coordinates were downloaded from the PDB database (PDB ID: 1RWT).

3. Results

3.1. Light-induced chlorophyll a fluorescence quenching in LHCII

Fig. 1 presents the time-dependencies of light-driven chlorophyll *a* fluorescence quenching induced by illumination with bright light. The light-driven fluorescence quenching in LHCII was slowly reversible and the fluorescence intensity reached ca. 30% of the initial level after the 20-min period of dark incubation following switching off of the illumination (not shown). Very similar reversibility of light-driven fluorescence quenching in LHCII has been reported by Barzda et al. [19]. Light-driven chlorophyll fluorescence quenching in LHCII was reversible by ca. 70% after the 60-min dark incubation, as reported originally by Jennings et al. [18] and in our previous reports [20,22,30]. Essential decrease in the average chlorophyll *a* fluorescence lifetimes, recorded after the exposure of the LHCII samples to strong light, has been observed (see Table 1). This effect indicates for the light-induced formation of excitation quenching centers. Chlorophyll *a* fluorescence emission spectra, recorded from the samples subjected to light-induced excitation quenching, were taken before and after the experiments, at room temperature and after decreasing temperature of the samples to 77 K.

3.2. Light-induced changes in the fluorescence emission spectra of chlorophyll a in LHCII, recorded at 77 K

Fig. 2 presents the comparison of the 77 K fluorescence emission spectra of chlorophyll *a* in LHCII, dark adapted and illuminated during the recording of the light-driven fluorescence quenching (as presented in Fig. 1). As can be seen, the process of light-induced fluorescence quenching in LHCII is associated with increase in intensity of the long-wavelength emission components, in particular the band in the

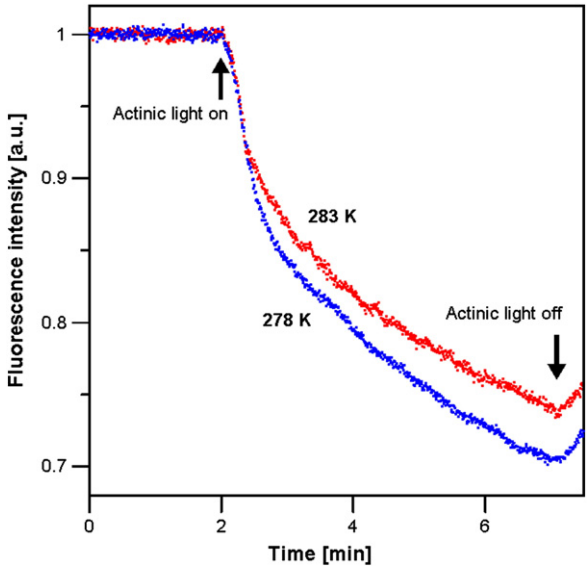

Fig. 1. Time courses of intensity of chlorophyll *a* fluorescence in LHCII embedded to lipid phase, excited with modulated light at 635 nm (0.18 μmol photons m^{-2} s^{-1}) and detected at 680 nm. Fluorescence quenching was induced by continuous actinic light 450 nm (500 μmol photons m^{-2} s^{-1}). Fluorescence dependencies were recorded at different temperatures, indicated. The fluorescence intensities were normalized at time zero.

spectral region close to 700 nm, relative to the principal band at 680 nm (see also Fig. S2 and Fig. S3 of the supplementary data). The 680 nm band is attributed to the fluorescence emission from the Q_y energy level of molecules of chlorophyll *a* bound to LHCII. The emission bands in the region of 700 nm represent the low-energy states, presumably of either chlorophyll *a* or chlorophyll *b*, which can accept excitation energy from all other LHCII-bound pigments with their lowest excited singlet energy levels located higher on energy scale. This band is characteristic of supramolecular structures of LHCII and therefore such a result can be interpreted in terms of light-induced reorganization of LHCII in

Table 1
Fluorescence lifetime analysis of LHCII incorporated into lipid membranes, dark adapted (dark) and illuminated with actinic blue light (450 nm, 500 μmol photons m^{-2} s^{-1}) for 5 min (light).

Excitation wavelength [nm]	Emission wavelength [nm]	Average fluorescence lifetime $\langle\tau\rangle$ [a] [ns]			
		Temperature [K]			
		300		77	
		Dark	Light	Dark	Light
470	680	1.01 (0.02)	0.83 (0.02)	1.61 (0.06)	1.12 (0.04)
	700	1.04 (0.02)	0.94 (0.01)	3.63 (0.05)	3.70 (0.06)
	740	1.07 (0.03)	1.01 (0.03)	1.56 (0.03)	1.46 (0.05)
642	680	1.21 (0.04)	1.09 (0.01)	1.57 (0.06)	1.34 (0.05)
	700	1.19 (0.04)	1.10 (0.02)	4.10 (0.06)	3.95 (0.05)
	740	1.26 (0.03)	1.14 (0.02)	1.94 (0.06)	1.83 (0.05)

[a] Amplitude weighted average fluorescence lifetime calculated according to formula: $\langle\tau\rangle = \Sigma\alpha_i\tau_i$ with the errors of evaluation (in parenthesis). Typically, the fluorescence decay kinetics at 300 K were fitted with three components characterized by the following lifetimes: $\tau_1 = 3.09$ ns, $\tau_2 = 1.14$ ns and $\tau_3 = 0.41$ ns, corresponding to trimeric LHCII and complexes organized into supramolecular structures [15,34]. Average fluorescence lifetimes are reported with the accuracy to the last significant digit. The lifetimes presented in the table were determined in the experiments carried out with the samples coming from one preparation. The initial (Dark) fluorescence lifetimes vary within the range of 20%, expressing different organization of LHCII in the samples coming from the different preparations, but the illumination and transfer to 77 K has the same effect in all the sample series examined, in terms of a change in lifetimes and amplitudes.

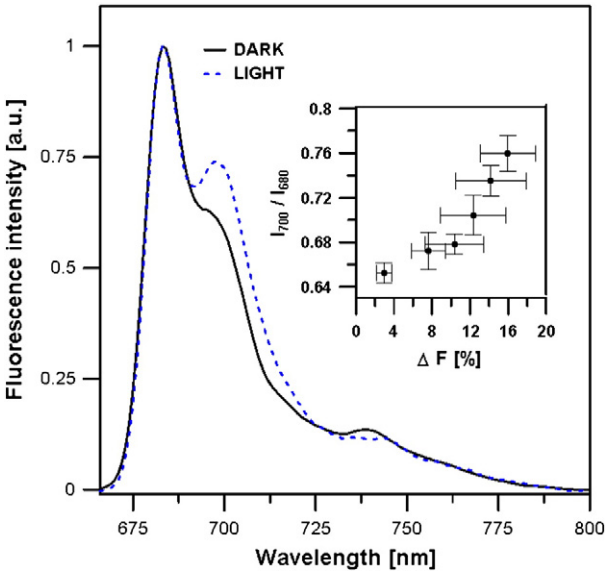

Fig. 2. The low temperature (77 K) chlorophyll *a* fluorescence emission spectra recorded from LHCII embedded in the lipid environment: solid black line — dark adapted and dashed blue line — illuminated (before the transfer to 77 K and the measurement) at room temperature for 5 min with blue light (450 nm, 500 μmol photons m^{-2} s^{-1}). The spectra were normalized at the maximum. Inset shows the relationship between the extent of fluorescence quenching (Δ*F*, calculated on the basis of the time dependencies as presented in Fig. 1) after different time periods (between 20 s and 5 min) versus the final ratio of fluorescence intensities at the maxima in the region of 700 nm and 680 nm (I_{700}/I_{680}). Experimental points represent arithmetic mean from 3 independent experiments (preparations) ± S.D.

the lipid environment, which results in higher aggregation level of the trimeric complex.

3.3. Chlorophyll a fluorescence lifetime analysis in LHCII

To test further photophysical properties of the low-energy emission bands fluorescence was subjected to the kinetic analysis (Table 1, see also Fig. S4 of the supplementary data). The fluorescence decay kinetics recorded show that LHCII embedded to a lipid phase, according to the procedure applied, appears in a partially aggregated form, as can be concluded on the basis of the shortened fluorescence lifetimes [15]. Such a molecular organization of the samples corresponds to the exceptionally high molecular crowding reported to appear in the thylakoid membranes of plants [31]. Moreover, it has been reported that the CD spectra of aggregated LHCII closely resemble those of thylakoid membranes, in contrast to the isolated complexes in the trimeric form [32]. Interestingly, the measurements taken at 77 K reveal that the emission at 700 nm is characterized by exceptionally long lifetimes, which contrasts with the other emission bands both at shorter and longer wavelengths: ~3 ns versus 1 ns. This is a clear indication that illumination of LHCII results in appearance of the long-wavelength spectral forms which are long-living and not subjected to excitation quenching. On the contrary, those energy levels can act as energy acceptors from the other states. The results of the experiments show clearly that either aggregation or illumination of LHCII, or both factors, lead to formation of the excitation quenching centers, associated with the emission bands centered in the region of 700 nm. On the other hand, it seems interesting why the long-wavelength emission bands which appear after illumination of LHCII are particularly visible in the fluorescence spectra recorded at low temperatures. To understand more deeply this problem we analyzed temperature dependencies of fluorescence spectra of chlorophyll *a* in LHCII.

3.4. Temperature dependencies of fluorescence spectra of chlorophyll a in LHCII

According to the general theory of photoluminescence [33] its integrated intensity I(T) depends on temperature according to the following equation:

$$I(T) = \frac{I_o}{1 + \kappa \exp(-E_a/RT)} \quad (1)$$

where *R* is an universal gas constant, I_o represents intensity at 0 K (for practical reasons often taken at any lowest recorded temperature, e.g. at 80 K, I_{80}), κ stands for the process rate parameter and E_a is an activation energy. Fig. 3 presents the analysis of temperature-dependencies of fluorescence emission of chlorophyll *a* in LHCII, in terms of Eq. (1) (the fluorescence emission spectra recorded at different temperatures are presented in Fig. S5). Owing to the fact that the fluorescence emission spectral components centered at 680 nm and at 700 nm may represent independent emitters the analysis presented in Fig. 3 has been performed for both the spectral forms separately, for the samples dark adapted and illuminated. As can be seen, the experiment cannot be described in a satisfactory manner by a single-linear dependency. The clear change of a slope of the linear dependencies, which appears in the region of 210 K, can be interpreted in terms of a structural transformation in the LHCII sample. Another observation is that the activation energies determined based on the fluorescence emission components at 680 nm are, in general, higher than those determined based on the fluorescence emission components at 700 nm. Additional observation is that the structural transition at 210 K is not as sharply pronounced in the illuminated sample as compared to the dark control.

Interestingly, a very distinctive discrepancy from the linear relationship, anticipated by the theory, can be noticed in the temperature region between 110 and 80 K, despite the fact that fluorescence intensity at each temperature has been corrected by the fluorescence emission intensity of the external standard in the same cryoprotective medium. This discrepancy can be also interpreted in terms of a structural transformation of the sample, which takes place in this particular temperature region and consumes selective excitation energy. This process results in the locally decreased fluorescence quantum yield and is manifested by positive deviation from the linear relationship in Fig. 3. The comparative FTIR analysis of LHCII at room temperature conditions and at 77 K revealed that the transition from higher to lower temperatures is associated with uncoupling of the vibrations assigned to the conjugated C═C bonds of the LHCII-bound pigments from the collective vibration modes of the protein [34]. It can be postulated that the same uncoupling is responsible for relatively high fluorescence quantum yield of chlorophyll forms emitting at 700 nm. It means that at physiological conditions the singlet excitation energy of this state is very efficiently quenched via inelastic absorption giving rise to protein collective vibrations. The temperature dependence of the relative intensity of the 700 nm band is presented in Fig. 4. On the other hand, relative increase in the fluorescence intensity at longer wavelengths (including at 700 nm) upon decrease in temperature, can be also interpreted in terms of the, so-called, Boltzmann population factors. Such an interpretation holds true assuming that the short-wavelength and the long-wavelength fluorescence emitters in LHCII samples are energetically coupled. This implies at least partial excitation quenching by the low-energy spectral forms.

3.5. Activation energy of the light-induced chlorophyll a fluorescence quenching in LHCII

The basic open question, regarding the mechanism of the light-driven excitation quenching in LHCII, which still requires to be addressed, relates to the molecular mechanism responsible for the

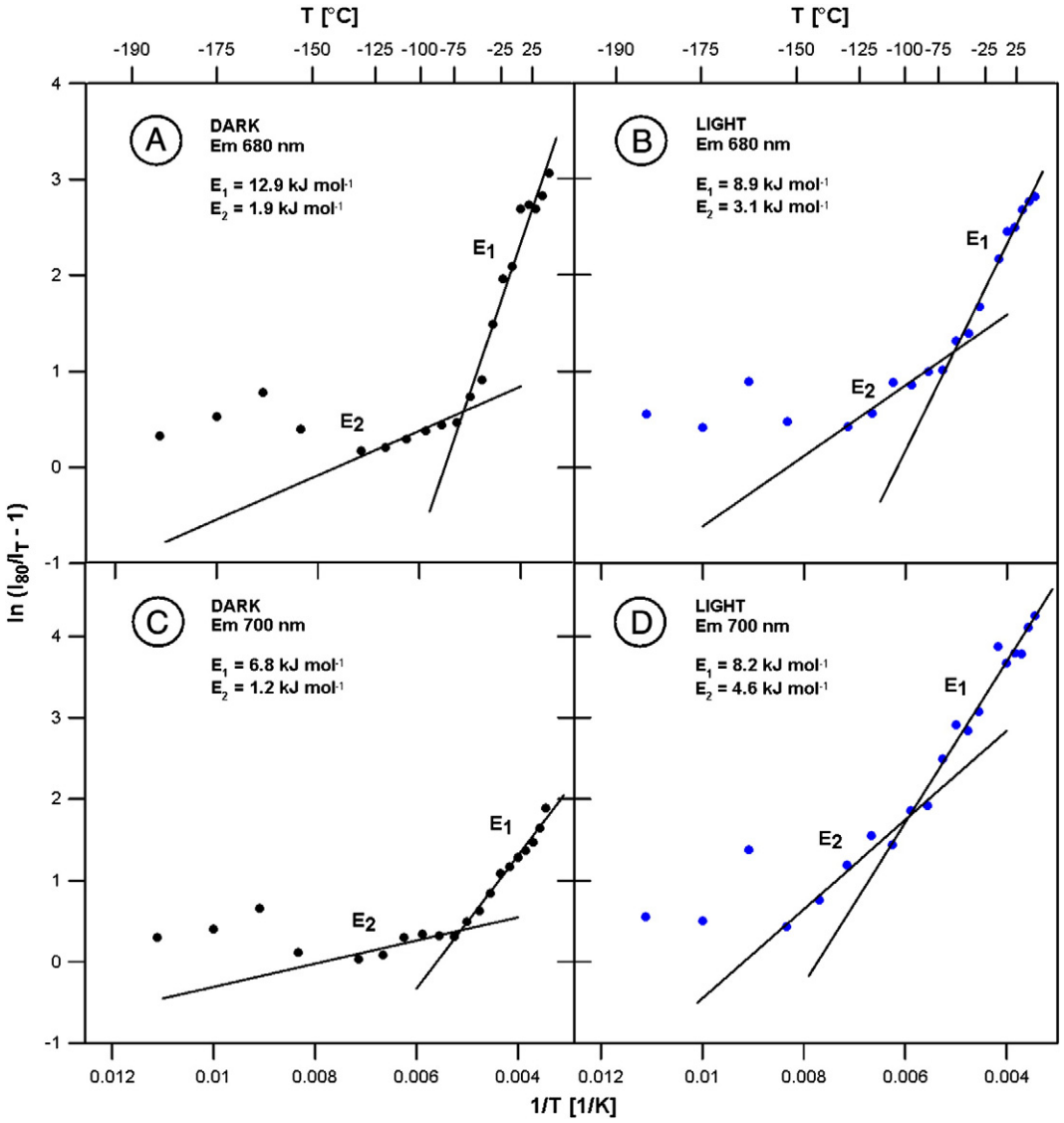

Fig. 3. Temperature dependencies of integrated intensities (I) of the Gaussian components at 680 nm and 700 nm, of fluorescence emission of chlorophyll *a* in LHCII samples excited at 642 nm. The solid black lines were fitted to the data points in the temperature range 290–200 K and 160–120 K. Before calculation of the logarithm each intensity was corrected (divided) by the integrated fluorescence intensity of Rhodamine 700 in the glycerol: water medium (2:1, v:v) recorded at the same temperature. Panels A and C represent measurements of the dark adapted samples while panels B and D represents the sample subjected before measurements to 5 min illumination (as in the case of the experiment presented in Fig. 1). Values of the activation energies (E_a) calculated on the basis of formula 1 and each of the linear fits are also presented.

formation of the 700 nm energy state. Fig. 5 presents the Arrhenius analysis of the second order rate constant of this process, fitted to the initial phase of a fluorescence decrease (assuming that the reversibility is negligible at the initial stage of quenching, owing to the relatively low concentration of quenching centers). Interestingly, the second order reaction approximation leads to the activation energies at a level characteristic of hydrogen bonds (-14.0 ± 3.7 kJ mol^{-1}). Moreover the activation energy has been determined negative in this temperature range, which means that the reaction is at least a two-step process with relatively high activation energy of the first step of reversibility. The exact energy barrier for the observed light-induced excitation quenching may be even higher due to the fact that the process observed is a result of a photo-reaction and the energy of low excited states can contribute to drive the reaction. The activation energy of the first order reaction, which was used to analyze the initial, fast component of the light-driven fluorescence quenching, has been determined by Barzda et al. to be 11.3 ± 0.9 kJ mol^{-1} [19]. The free energy difference at room temperature, of the chlorophyll *a* fluorescence quenching in LHCII, evoked by the protein aggregation induced by dissolving trimeric protein in a buffer containing the detergent in a concentration lower than the critical micellar concentration, has been determined by Santabarbara et al. as 7.0 kJ mol^{-1} [35] and is relatively close to the energies determined in the case of light-driven processes. This observation suggests similar origin of those two phenomena, induced by illumination and protein aggregation.

FTIR analysis shows that illumination of LHCII, resulting in the excitation quenching, is associated with the spectral shift towards higher frequencies, of the band representing the C—OH stretching vibrations (Fig. 6). Such a shift can be interpreted as resulting from light-induced processes of breaking hydrogen bonds in which the C—OH groups are involved, e.g. with involvement of the LHCII bound xanthophylls. At the same time, no major spectral shifts have been observed in the principal IR absorption band corresponding to the protein vibrations (see Fig. S6): the amide I band (between 1600 and 1700 cm^{-1}). On the other hand, the analysis of the amide I band shows that illumination of LHCII sample results in change in the molecular organization status of the protein: increase in the spectral components which can be attributed to protein aggregation [34].

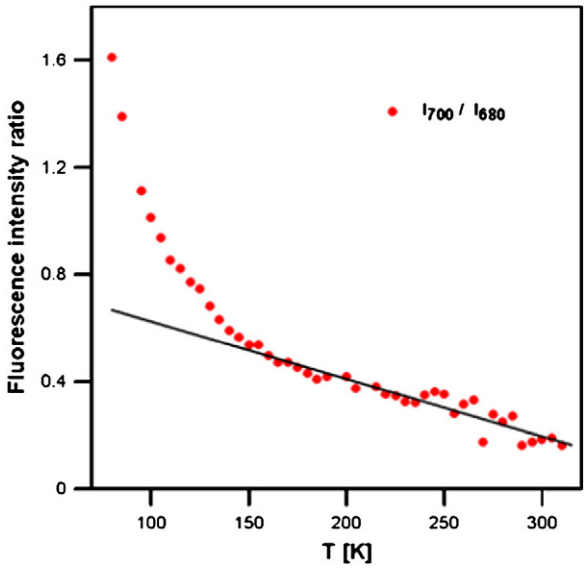

Fig. 4. Temperature dependency of the fluorescence intensity ratio of a spectral band at 700 nm to a band at 680 nm in the chlorophyll *a* emission spectrum in LHCII (dark adapted). The excitation was set at 642 nm. The ratio was calculated on the basis of integrated Gaussian components centered in the region of 700 and 680 nm. The Gaussian components of deconvolution of the emission spectra were as the ones presented in Fig. S2. The solid black line was fitted to the 31 data points in the temperature range 150–310 K ($R^2 = 0.92$).

3.6. Low-temperature fluorescence emission spectra of LHCII with reduced neoxanthin content

Light-induced fluorescence quenching in LHCII has been shown recently to be accompanied by photo-isomerization of neoxanthin in the complex [36]. It was postulated that such an isomerization can lead to formation of supramolecular structures of LHCII out of trimers [36]. In order to study possible relationship between the appearance of the long-wavelength emission bands and neoxanthin content we have elaborated the procedure which yields partial and selective extraction of neoxanthin from the complex. Fig. 7 presents the 77 K fluorescence emission spectrum of the LHCII sample with reduced neoxanthin content. The samples were excited at 470 nm, in the spectral region corresponding to the light absorption by the LHCII-bound xanthophylls and chlorophyll *b*. The appearance of a relatively weak emission band at 654 nm, attributed to the fluorescence emission from chlorophyll *b*, indicates that the excitation energy transfer to chlorophyll *a*, in the system studied, is not 100% efficient. Interestingly, selective extraction of neoxanthin results in a decrease of the intensity of this particular emission band and concomitant appearance of the long-wavelength emission bands which can be attributed to spectral forms of aggregated LHCII. The spectral effects accompanying partial extraction of neoxanthin are also associated with a slight decrease of the amplitude weighted average fluorescence lifetimes (296 K, excitation at 470 nm, observation at 700 nm): from 1.28 ± 0.01 ns to 1.08 ± 0.01 ns.

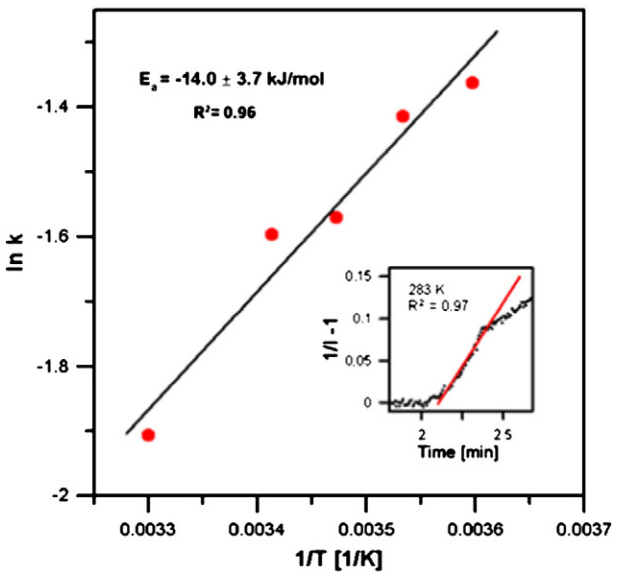

Fig. 5. Arrhenius analysis of the chlorophyll *a* fluorescence intensity decrease induced by actinic blue light (450 nm, as presented in Fig. 1), measured at the range of temperatures: 278–303 K. Activation energy for a quenching was calculated according to the equation: $\ln k = \ln A - E_a/RT$. Reaction rate constants (k) were determined as a slope of the linear function fitted to the experimental points corresponding to the initial phase of fluorescence decrease (time between 2.1 min and 2.4 min) of each decay converted to the function $1/I - 1 = kt$ which represents the initial phase of the second order reaction, assuming negligibly low reversibility due to the low concentration of the quenched form (see the insert for the method of calculation).

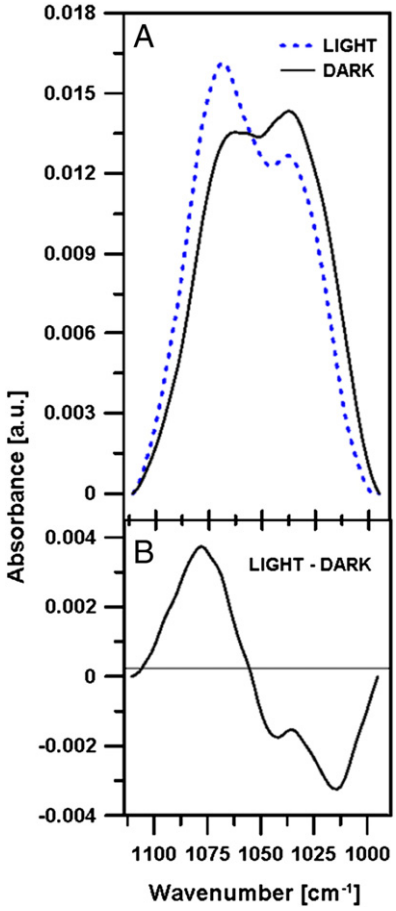

Fig. 6. The 77 K infrared absorption spectra of LHCII samples in the spectral region corresponding to the C-OH stretching vibrations: dark adapted (solid black line, DARK) and illuminated before the measurement for 10 minutes with blue light (450 nm, 500 μmol photons m^{-2} s^{-1}; dashed blue line, LIGHT). Spectra were normalized to get the same integrated area beneath each spectrum. Lower panel presents the difference spectrum showing the effect of the illumination.

4. Discussion

In this work we show that illumination of LHCII, embedded in the chloroplast lipid environment, results in increase of intensity of the fluorescence emission band in the region of 700 nm, relative to the

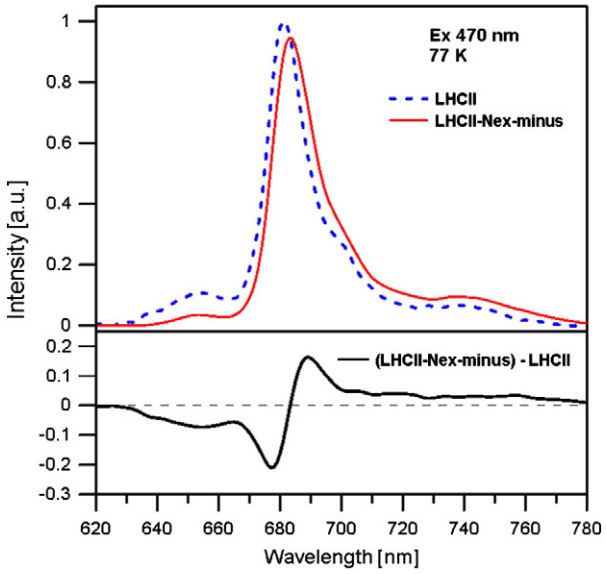

Fig. 7. 77 K chlorophyll fluorescence emission spectra recorded from LHCII embedded in the lipid environment: solid red line — sample with reduced neoxanthin content (0.88 neoxanthin per 2 lutein) and the control sample: dashed blue line (1.01 neoxanthin per 2 lutein). The spectra were normalized with respect to the surface area beneath each spectrum. The lower panel shows the difference spectrum. The maximum of the difference spectrum appears at 690 nm.

principal band at 680 nm (in the spectra recorded at 77 K). The fact that appearance of this particular state is correlated with the initial phase of excitation quenching in LHCII makes questions regarding its nature not only interesting but also important. The illumination of LHCII and appearance of the 700 nm band in the low-temperature fluorescence emission spectra of chlorophyll *a* in LHCII (detected at 680 nm) is also associated with a certain shortening of the average fluorescence lifetime. As can be seen from Table 1, illumination for 5 min. of the LHCII sample at room temperature results in a decrease of the average fluorescence lifetime parameter (excited at 470 nm and monitored at 680 nm) from 1.01 to 0.83 ns (by ca. 18 %). On the other hand, the same illumination results in a decrease of the fluorescence signal by ca. 20 %. In our opinion the correspondence is fairly good and the slightly lower quenching effect, as pronounced by the average fluorescence lifetime decrease, indicates that we are not dealing with the dynamic excitation quenching (as for example due to collisions with O_2) but rather with a mixture of the static effect (association of the quencher with the fluorophore in the ground state) and excitation energy transfer to a quencher. Owing to the fact that quenched excitations do not give rise to fluorescence signal and therefore they are not detected by the time-correlated single photon counting instrumentation, apparent fluorescence lifetime can be less affected, despite efficient operation of excitation quenching. For example, similar effect was observed in the FLIM (Fluorescence Lifetime Imaging Microscopy) analysis of the LHCII samples in which the chlorophyll fluorescence was quenched by incorporation of the exogenous xanthophylls which affected molecular organization of the protein [37]. Imaging of the heterogeneous samples enabled detection of the areas characterized by the efficient fluorescence quenching and simultaneously characterized by very low number of emitted quanta, with very low contribution to overall fluorescence lifetime analysis.

The 700 nm band is exclusively observed at low temperatures in samples composed of aggregated LHCII [38]. The analysis of the emission band at 700 nm has been widely applied to monitor molecular organization of LHCII and formation of oligomeric structures [9,38–40]. This band has been also considered as an artifact coming from distortion of the chlorophyll *a* emission spectra due to fluorescence reabsorption in bulk LHCII aggregates [6]. On the other hand, the presence of this band in the emission spectra recorded from single LHCII monolayers [34] supports the interpretation according to which this is a real emission band representing the individual energy state. The intensity of this particular band increases in course of illumination of LHCII, not only relatively to the fluorescence emission band at 680 nm but also on the absolute scale. This can be seen, for example, in Fig. S7 of the supplementary data. This means that illumination of LHCII results in appearance of the new spectral form which gives rise to fluorescence emission in the region of 700 nm at 77 K. Interestingly, as can be seen from the fluorescence emission spectra (e.g. Fig. 2, Fig. S2, Fig. S3), the appearance of the 700 nm band is associated with the chlorophyll fluorescence quenching in the spectral regions both corresponding to higher energies but also those which appear at longer wavelengths. This is demonstrated by an overlap of the normalized emission spectra in the region of the band at 680 nm and above 725 nm. This effect is an indication that the relatively broad emission band at 700 nm represents the state able to quench efficiently singlet excitations also from the pigment molecules with singlet excited states located on energy scale slightly below. The relatively high width of the emission band centered in the region of 700 nm (FWHH higher than 20 nm, see Fig. S2) with respect to the band centered in the region of 680 nm (FWHH 10 nm) seems to be in agreement with the interpretation that this band contains significant contribution from charge transfer state. The distinctive signature of this state is also a much longer fluorescence lifetime determined at 77 K ($<\tau>=3.7$ ns at 700 nm) as compared to the emission at 680 nm ($<\tau>=1.12$ ns) and emission at 740 nm ($<\tau>=1.46$ ns, see Table 1 and Fig. S4).

Recently, we reported the light-induced isomerization of the xanthophyll neoxanthin, both in solution and bound to LHCII [36]. The photo-isomerization of neoxanthin has been concluded to be a reaction which can be mediated by the excited triplet state of the carotenoid [36] and therefore can be photo-sensitized by chlorophylls. Photo-isomerization of neoxanthin has been shown to result in transformation of the 9′-*cis* molecular configuration to the di-*cis* forms (9′,13′ and 9′13), which are not able to form inter-trimer links via the hydrogen bonds between the hydroxyl groups located in the positions C3 and C5 (see Fig. 8). Neoxanthin molecular configuration 9′-*cis* has lower energy than the di-*cis* forms therefore the process is spontaneously reversible [36]. Neoxanthin is the only xanthophyll molecule protruding outside the LHCII structure, on the one hand, and possessing relatively high molecular motion freedom, represented by the crystallographic temperature factors [41] on the other hand. It seems therefore very likely that under physiological conditions, hydrogen bridges between the neoxanthin ends sticking out of the neighboring LHCII complexes (trimers), stabilize the supramolecular structure. In principle, hydrogen bonds between the hydroxyl groups of neoxanthin can stabilize two, essentially different structures, presented in Fig. 8. Very important feature of such a structure, in terms of excitation quenching in LHCII, is that formation of hydrogen bond bridges between the neoxanthin molecules either prevents or promotes a very close contact between chlorophylls located at the periphery of neighboring complexes, such as chlorophyll *b* located directly below neoxanthin (Chl 14 in the terminology of Standfuss et al. [6] or 605 in the terminology of Liu et al. [3]). Two states of the supramolecular organization of the complex are shown: the energy conserving and the energy dissipative states. The states are characterized by a different strength of the hydrogen bonds between the hydroxyl groups of the neoxanthin molecules anchored in the neighboring LHCII trimers: the relatively strong hydrogen bond between the hydroxyl groups at the C3 positions (the distance between the oxygen atoms lower than 0.25 nm, referred to as the antenna active state) and the relatively weak hydrogen bond between the hydroxyl groups at the C5 positions (the distance between the oxygen atoms longer than 0.30 nm, referred to as the energy dissipative state). The transition between the states requires breaking of the hydrogen bonds, which can be realized via the neoxanthin photo-isomerization

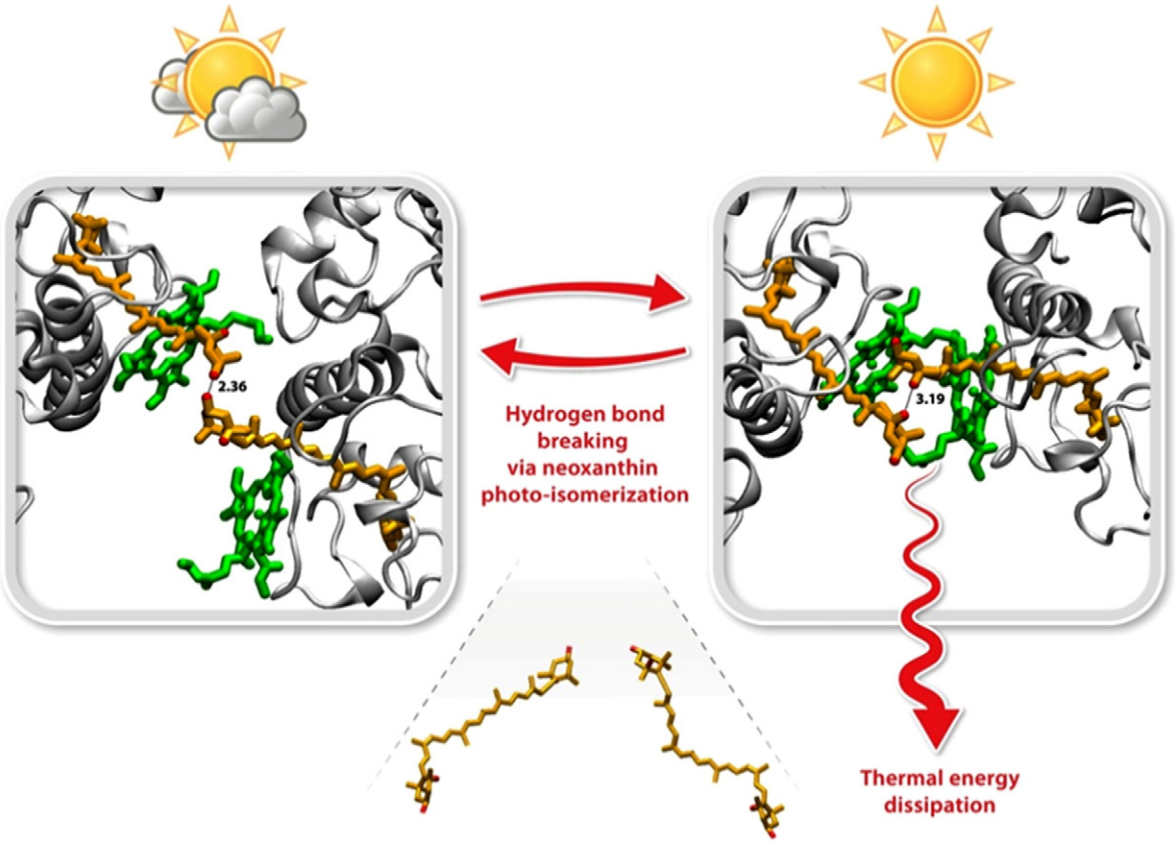

Fig. 8. The model of the light-controlled molecular mechanism which regulates excitation level in the photosynthetic complex LHCII. Presented are the top views of the contact regions between the neighboring LHCII complexes with indicated hydrogen bonds which can be potentially formed between the hydroxyl groups of the neoxanthin molecules anchored in the complexes forming a supramolecular structure. See the text for more explanation. Interaction of LHCII trimers was analyzed and visualized with VMD software support (http://www.ks.uiuc.edu/Research/vmd/). LHCII coordinates were downloaded from the PDB database (PDB ID: 1RWT).

pathway: 9′-*cis* → 9′,13-di-*cis* → 9′-*cis* [36]. Due to the higher activation energy, the transition to the dissipative state requires higher energy as compared to the reversibility to the physiological, light harvesting state. The concept on light-induced breaking of the hydrogen bonds between neoxanthin molecules and its relationship with excitation quenching has strong support from the activation energy and FTIR analyses presented in this work.

Very recently, it was shown that formation of the photoprotective state in plants requires a structural reorganization of the photosynthetic membrane involving aggregation of LHCII [42]. Such a mechanism agrees with the concept according to which aggregated structures of LHCII play important physiological role both, in physiological and light stress conditions [43,44]. On the other hand, the model studies have shown that aggregation of light-harvesting complex II leads to formation of efficient excitation energy traps in monomeric and trimeric complexes [15]. Aggregation of LHCII creates natural conditions of a close contact of chlorophyll molecules located at the periphery of individual complexes both in the monomeric and trimeric forms. The formation of the charge transfer complexes by two peripherally located molecules Chl 14 has been postulated to create the energy trap responsible for excitation quenching in LHCII [36]. Activity of charge transfer complexes as energy dissipation centers in LHCII has been originally postulated by Miloslavina et al. [9]. Very recently, it was shown, that the charge transfer complexes give rise to intensity of the fluorescence emission band in the region of 700 nm [10], which provides a strong support to the interpretation presented in this paper. Analysis of the supramolecular structure presented in Fig. 8, referred to as the energy dissipative state, shows that the molecules Chl 14 remain in the van der Waals contact and can be involved in formation of a charge transfer complex.

Neoxanthin is a unique pigment in the sense that it is bound to the protein and at the same time it is present in the lipid phase of the thylakoid membrane. Owing to such a localization the pigment is able to neutralize reactive oxygen species much more efficiently than other xanthophylls, such as lutein, incorporated more deeply into the protein [45]. Such a localization of neoxanthin has also the consequences in the supramolecular organization of LHCII. According to our understanding xanthophyll molecule in the N1 binding site is not necessary to develop aggregation of LHCII and excitation quenching but, on the contrary, it hinders close contact of the protein subunits in the place of binding of the peripheral chlorophyll *b* referred to as Chl 14. According to this, we expect even higher aggregation level of LHCII under the absence of xanthophyll in the neoxanthin-binding pocket. Fig. 7 presents the spectroscopic evidence that partial removal of neoxanthin from the LHCII preparation results in higher aggregation level of the protein, as demonstrated by the intensity of the long-wavelength spectral bands, in particularly in the region of 700 nm. Interestingly, the intensity of this low-energy band is apparently inversely proportional to the intensity of the emission band at 654 nm, attributed to chlorophyll *b*. Such a correlation corroborates the interpretation according to which the low-energy band originates from aggregation of chlorophyll *b* molecules. The extraction procedure applied removes approximately 10% of neoxanthin from LHCII. We have also tested extraction with higher concentration of pentane and we have found that such a procedure resulted in extraction of higher fractions of neoxanthin. On the other hand, in such cases we also detected partial extraction of violaxanthin and chlorophylls. Therefore we decided to analyze exclusively the data obtained with the preparation with selectively extracted neoxanthin. In such a case

the effect on the fluorescence emission spectra is not very strong but the direction of changes observed remains in perfect agreement with the model discussed. According to this model, neoxanthin remains anchored in its N1 binding site, under the physiological conditions, but light-driven isomerization of this pigment can control formation of LHCII aggregated structures in which peripheral molecules of chlorophyll *b* (Chl 14) are close enough to give rise to an excitonic pair or a charge transfer complex.

5. Conclusions

Here, we report that light-driven singlet excitation quenching in LHCII, manifested by decrease in the chlorophyll *a* fluorescence intensity and by shortening of the fluorescence lifetimes, is associated with appearance of the new, low-energy state corresponding to emission in the region of 700 nm. Fluorescence emission from this particular state is particularly observed at low temperatures (77 K) and the energy of this state is effectively dissipated via the phonon transfer to the apoprotein environment and assimilated via collective protein motion at physiological temperatures. This channel of energy dissipation is, to a large extent, uncoupled at 77 K, following the structural transformations of the protein observed at low temperatures. The energy state associated with excitation quenching presents individual decay kinetics characterized by essentially longer lifetimes, at 77 K. Light-induced excitation quenching in LHCII has an activation energy at the level corresponding to energy of hydrogen bonds. The activation of the transitions between the antenna active and the energy dissipative states has been interpreted in terms of breaking of the hydrogen bonds between the hydroxyl groups of neoxanthin molecules anchored in the neighboring complexes, as based on the FTIR analysis and literature data regarding the photo-isomerization of neoxanthin. The energy dissipative state has been interpreted as originating from a supramolecular structure of LHCII which enables closer contact of individual trimers and formation of low-energy charge transfer complexes by peripheral chlorophyll molecules (presumably chlorophyll b: Chl 14). This hypothetical molecular mechanism is one of several which can potentially act to regulate down the excitation density in the photosynthetic antenna LHCII in the photosynthetic apparatus subjected to light stress.

Acknowledgments

This research has been performed within the framework of the project “Molecular Spectroscopy for BioMedical Studies” financed by the Foundation for Polish Science within the TEAM program.

Appendix A. Supplementary data

Supplementary data to this article can be found online at http://dx.doi.org/10.1016/j.bbabio.2012.11.013.

References

[1] M.F. Hohmann-Marriott, R.E. Blankenship, Evolution of photosynthesis, Annu. Rev. Plant Biol. 62 (2011) 515–548.
[2] W. Kühlbrandt, Structure and function of the plant light-harvesting complexes, LHC-II, Curr. Opin. Struct. Biol. 4 (1994) 519–528.
[3] Z. Liu, H. Yan, K. Wang, T. Kuang, J. Zhang, L. Gui, X. An, W. Chang, Crystal structure of spinach major light-harvesting complex at 2.72 A resolution, Nature 428 (2004) 287–292.
[4] M.G. Muller, P. Lambrev, M. Reus, E. Wientjes, R. Croce, A.R. Holzwarth, Singlet energy dissipation in the photosystem II light-harvesting complex does not linvolve energy transfer to carotenoids, Chem. Phys. Chem. 11 (2010) 1289–1296.
[5] A.V. Ruban, M.P. Johnson, C.D.P. Duffy, The photoprotective molecular switch in the photosystem II antenna, Biochim. Biophys. Acta-Bioenerg. 1817 (2012) 167–181.
[6] R. Standfuss, A.C.T. van Scheltinga, M. Lamborghini, W. Kuhlbrandt, Mechanisms of photoprotection and nonphotochemical quenching in pea light-harvesting complex at 2.5A resolution, EMBO J. 24 (2005) 919–928.
[7] T.K. Ahn, T.J. Avenson, M. Ballottari, Y.C. Cheng, K.K. Niyogi, R. Bassi, G.R. Fleming, Architecture of a charge-transfer state regulating light harvesting in a plant antenna protein, Science 320 (2008) 794–797.
[8] N.E. Holt, D. Zigmantas, L. Valkunas, X.P. Li, K.K. Niyogi, G.R. Fleming, Carotenoid cation formation and the regulation of photosynthetic light harvesting, Science 307 (2005) 433–436.
[9] Y. Miloslavina, A. Wehner, P.H. Lambrev, E. Wientjes, M. Reus, G. Garab, R. Croce, A.R. Holzwarth, Far-red fluorescence: a direct spectroscopic marker for LHCII oligomer formation in non-photochemical quenching, FEBS Lett. 582 (2008) 3625–3631.
[10] M. Wahadoszamen, R. Berera, A.M. Ara, E. Romero, R. van Grondelle, Identification of two emitting sites in the dissipative state of the major light harvesting antenna, Phys. Chem. Chem. Phys. 14 (2012) 759–766.
[11] A.V. Ruban, R. Berera, C. Ilioaia, I.H. van Stokkum, J.T. Kennis, A.A. Pascal, H. van Amerongen, B. Robert, P. Horton, R. van Grondelle, Identification of a mechanism of photoprotective energy dissipation in higher plants, Nature 450 (2007) 575–578.
[12] T. Barros, W. Kuhlbrandt, Crystallisation, structure and function of plant light-harvesting Complex II, Biochim. Biophys. Acta-Bioenerg. 1787 (2009) 753–772.
[13] G.S. Beddard, G. Porter, Concentration quenching in chlorophyll, Nature 260 (1976) 366–367.
[14] B. van Oort, A. van Hoek, A.V. Ruban, H. van Amerongen, Equilibrium between quenched and nonquenched conformations of the major plant light-harvesting complex studied with high-pressure time-resolved fluorescence, J. Phys. Chem. B 111 (2007) 7631–7637.
[15] B. van Oort, A. van Hoek, A.V. Ruban, H. van Amerongen, Aggregation of light-harvesting complex II leads to formation of efficient excitation energy traps in monomeric and trimeric complexes, FEBS Lett. 581 (2007) 3528–3532.
[16] C. Ilioaia, M.P. Johnson, P. Horton, A.V. Ruban, Induction of efficient energy dissipation in the isolated light-harvesting complex of Photosystem II in the absence of protein aggregation, J. Biol. Chem. 283 (2008) 29505–29512.
[17] T.P.J. Kruger, V.I. Novoderezhkin, C. Ilioaia, R. van Grondelle, Fluorescence spectral dynamics of single LHCII trimers, Biophys. J. 98 (2010) 3093–3101.
[18] R. Jennings, F. Garlaschi, G. Zucchelli, Light-induced fluorescence quenching in the light-harvesting chlorophyll a/b protein complex, Photosynth. Res. 27 (1991) 57–64.
[19] V. Barzda, R.C. Jennings, G. Zucchelli, G. Garab, Kinetic analysis of the light-induced fluorescence quenching in light-harvesting chlorophyll a/b pigment–protein complex of photosystem II, Photochem. Photobiol. 70 (1999) 751–759.
[20] W. Grudzinski, Z. Krupa, M. Garstka, W. Maksymiec, T.E. Swartz, W.I. Gruszecki, Conformational rearrangements in light-harvesting complex II accompanying light-induced chlorophyll a fluorescence quenching, Biochim. Biophys. Acta 1554 (2002) 108–117.
[21] W.I. Gruszecki, W. Grudzinski, M. Matula, P. Kernen, Z. Krupa, Light-induced excitation quenching and structural transition in light-harvesting complex II, Photosynth. Res. 59 (1999) 175–185.
[22] W.I. Gruszecki, P. Kernen, Z. Krupa, R.J. Strasser, Involvement of xanthophyll pigments in regulation of light-driven excitation quenching in light-harvesting complex of Photosystem II, Biochim. Biophys. Acta 1188 (1994) 235–242.
[23] Z. Krupa, N. Huner, J. Williams, E. Maissan, D. James, Development at cold-hardening temperatures. The structure and composition of purified rye light harvesting complex II, Plant Physiol. 84 (1987) 19–24.
[24] W.I. Gruszecki, M. Gospodarek, W. Grudzinski, R. Mazur, K. Gieczewska, M. Garstka, Light-induced change of configuration of the LHCII-bound xanthophyll (tentatively assigned to violaxanthin): a resonance Raman study, J. Phys. Chem. B 113 (2009) 2506–2512.
[25] I. Simidjiev, V. Barzda, L. Mustardy, G. Garab, Isolation of lamellar aggregates of the light-harvesting chlorophyll a/b protein complex of photosystem II with long-range chiral order and structural flexibility, Anal. Biochem. 250 (1997) 169–175.
[26] I. Simidjiev, V. Barzda, L. Mustardy, G. Garab, Role of thylakoid lipids in the structural flexibility of lamellar aggregates of the isolated light-harvesting chlorophyll a/b complex of photosystem II, Biochemistry 37 (1998) 4169–4173.
[27] W. Grudzinski, M. Matula, J. Sielewiesiuk, P. Kernen, Z. Krupa, W.I. Gruszecki, Effect of 13-cis violaxanthin on organization of light harvesting complex II in monomolecular layers, Biochim. Biophys. Acta 1503 (2001) 291–302.
[28] M. Gagos, J. Gabrielska, M. Dalla Serra, W.I. Gruszecki, Binding of antibiotic amphotericin B to lipid membranes: monomolecular layer technique and linear dichroism-FTIR studies, Mol. Membr. Biol. 22 (2005) 433–442.
[29] W. Humphrey, A. Dalke, K. Schulten, VMD — visual molecular dynamics, J. Mol. Graphics 14 (1996) 33–38.
[30] W.I. Gruszecki, M. Zubik, R. Luchowski, W. Grudzinski, M. Gospodarek, J. Szurkowski, Z. Gryczynski, I. Gryczynski, Investigation of the molecular mechanism of the blue-light-specific excitation energy quenching in the plant antenna complex LHCII, J. Plant Physiol. 168 (2011) 409–414.
[31] S. Haferkamp, W. Haase, A.A. Pascal, H. van Amerongen, H. Kirchhoff, Efficient light harvesting by photosystem II requires an optimized protein packing density in grana thylakoids, J. Biol. Chem. 285 (2010) 17020–17028.
[32] P.H. Lambrev, Z. Varkonyi, S. Krumova, L. Kovacs, Y. Miloslavina, A.R. Holzwarth, G. Garab, Importance of trimer–trimer interactions for the native state of the plant light-harvesting complex II, Biochim. Biophys. Acta 1767 (2007) 847–853.
[33] J. Krustok, H. Collan, K. Hjelt, Does the low-temperature Arrhenius plot of the photoluminescence intensity in CdTe point towards an erroneous activation energy? J. Appl. Phys. 81 (1997) 1442–1445.
[34] W.I. Gruszecki, E. Janik, R. Luchowski, P. Kernen, W. Grudzinski, I. Gryczynski, Z. Gryczynski, Supramolecular organization of the main photosynthetic antenna complex LHCII: a monomolecular layer study, Langmuir 25 (2009) 9384–9391.

[35] S. Santabarbara, P. Horton, A.V. Ruban, Comparison of the thermodynamic landscapes of unfolding and formation of the energy dissipative state in the isolated light harvesting complex II, Biophys. J. 97 (2009) 1188–1197.
[36] M. Zubik, R. Luchowski, W. Grudzinski, M. Gospodarek, I. Gryczynski, Z. Gryczynski, J.W. Dobrucki, W.I. Gruszecki, Light-induced isomerization of the LHCII-bound xanthophyll neoxanthin: possible implications for photoprotection in plants, Biochim. Biophys. Acta 1807 (2011) 1237–1243.
[37] W.I. Gruszecki, M. Zubik, R. Luchowski, E. Janik, W. Grudzinski, M. Gospodarek, J. Goc, L. Fiedor, Z. Gryczynski, I. Gryczynski, Photoprotective role of the xanthophyll cycle studied by means of modeling of xanthophyll–LHCII interactions, Chem. Phys. 373 (2010) 122–128.
[38] A.V. Ruban, J.P. Dekker, P. Horton, R. van Grondelle, Temperature-dependence of chlorophyll fluorescence from the light-harvesting complex II of higher plants, Photochem. Photobiol. 61 (1995) 216–221.
[39] W.I. Gruszecki, M. Matula, B. Mysliwa-Kurdziel, P. Kernen, Z. Krupa, Z. Strzalka, Effect of xanthophyll pigments on fluorescence of chlorophyll a in LHC II embedded to liposomes, J. Photochem. Photobiol. B 37 (1997) 84–90.
[40] A.V. Ruban, D. Rees, A.A. Pascal, P. Horton, Mechanism of delta pH-dependent dissipation of absorbed excitation energy by photosynthetic membranes. II. The relationship between LHCII aggregation in vitro and qE in isolated thylakoids, Biochim. Biophys. Acta 1102 (1992) 39–44.
[41] T. Barros, A. Royant, J. Standfuss, A. Dreuw, W. Kuhlbrandt, Crystal structure of plant light-harvesting complex shows the active, energy-transmitting state, EMBO J. 28 (2009) 298–306.
[42] M.P. Johnson, T.K. Goral, C.D.P. Duffy, A.P.R. Brain, C.W. Mullineaux, A.V. Ruban, Photoprotective energy dissipation involves the reorganization of photosystem II light-harvesting complexes in the grana membranes of spinach chloroplasts, Plant Cell 23 (2011) 1468–1479.
[43] P. Horton, A.V. Ruban, D. Rees, A.A. Pascal, G. Noctor, A.J. Young, Control of the light-harvesting function of chloroplast membranes by aggregation of the LHCII chlorophyll–protein complex, FEBS Lett. 292 (1991) 1–4.
[44] V. Barzda, A. Istokovics, I. Simidjiev, G. Garab, Structural flexibility of chiral macroaggregates of light-harvesting chlorophyll a/b pigment–protein complexes. Light-induced reversible structural changes associated with energy dissipation, Biochemistry 35 (1996) 8981–8985.
[45] L. Dall'Osto, S. Cazzaniga, H. North, A. Marion-Poll, R. Bassi, The *Arabidopsis* aba4-1 mutant reveals a specific function for neoxanthin in protection against photooxidative stress, Plant Cell 19 (2007) 1048–1064.